

Supporting Information

Synergistic Effect of Alloying on Thermoelectric Properties of Two-Dimensional PdP Q ($Q=S, Se$)

Shima Shahabfar¹, Yi Xia², M. Hossein Morshedsolouk¹, Mahsa Mohammadi
Bidhendi¹, and S. Shahab Naghavi^{1*}

¹Department of Physical and Computational Chemistry, Shahid Beheshti University, Tehran
1983969411, Iran

²Department of Mechanical and Materials Engineering, Portland State University, Portland, Oregon,
97201, USA

E-mail: s_naghavi@sbu.ac.ir

Compound	a	b	BG _{PBE}	BG _{HSE}	BG _{SOC}	ϵ_{∞}^{xx}	ϵ_{∞}^{yy}	P—P Dissociation Energy (eV)
PdPS	5.698	7.731	1.19	2.16	1.1929	4.22	4.28	1.67
PdPSe	5.846	5.902	1.1164	2.012	1.098	4.64	4.75	1.72

Table S1: Lattice parameters(Å), band gaps in eV(PBE, HSE, and spin orbit coupling included) and infinite dielectric constants for PdPSe and PdPS monolayers.

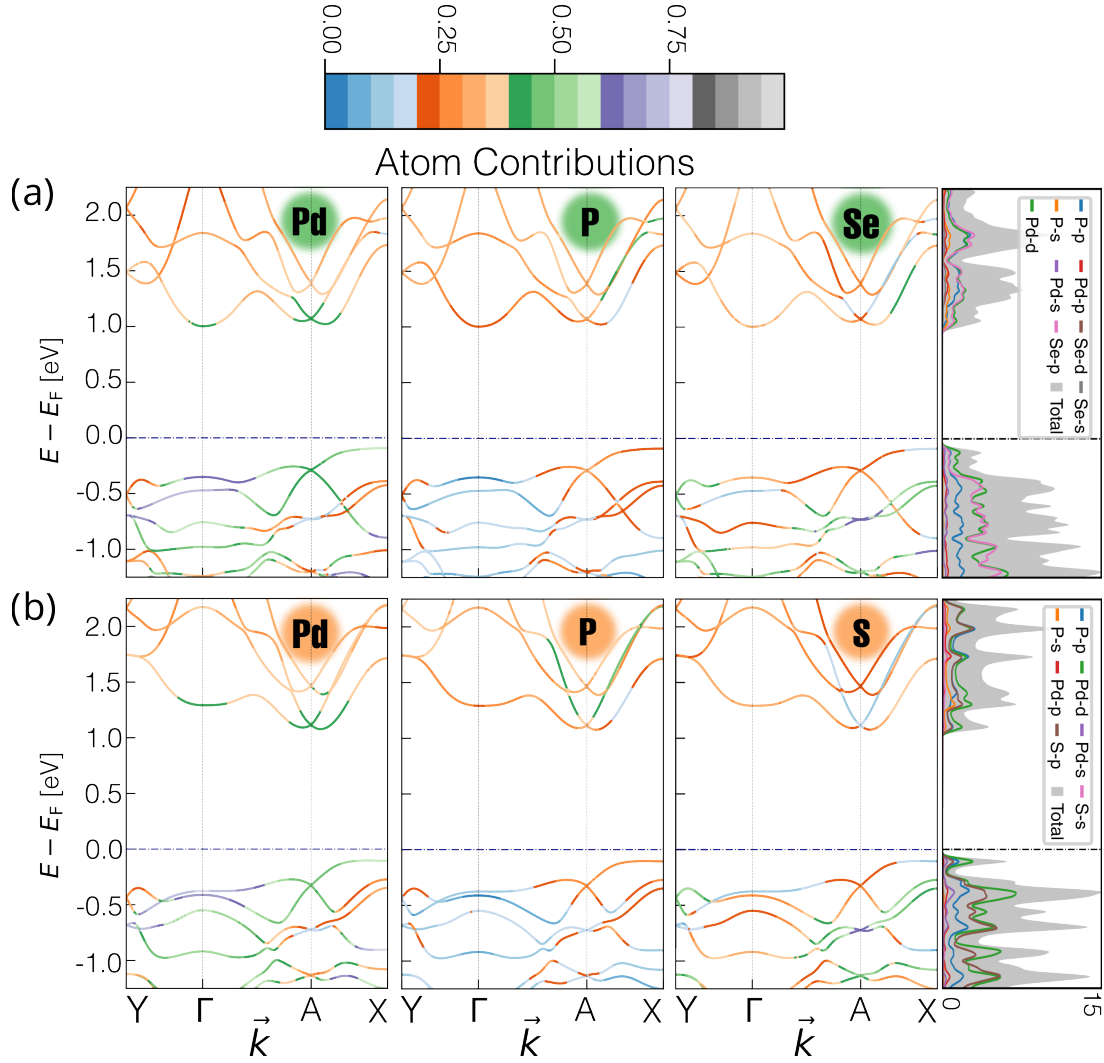


Fig. S1: Atom projected band structures of PdPSe .

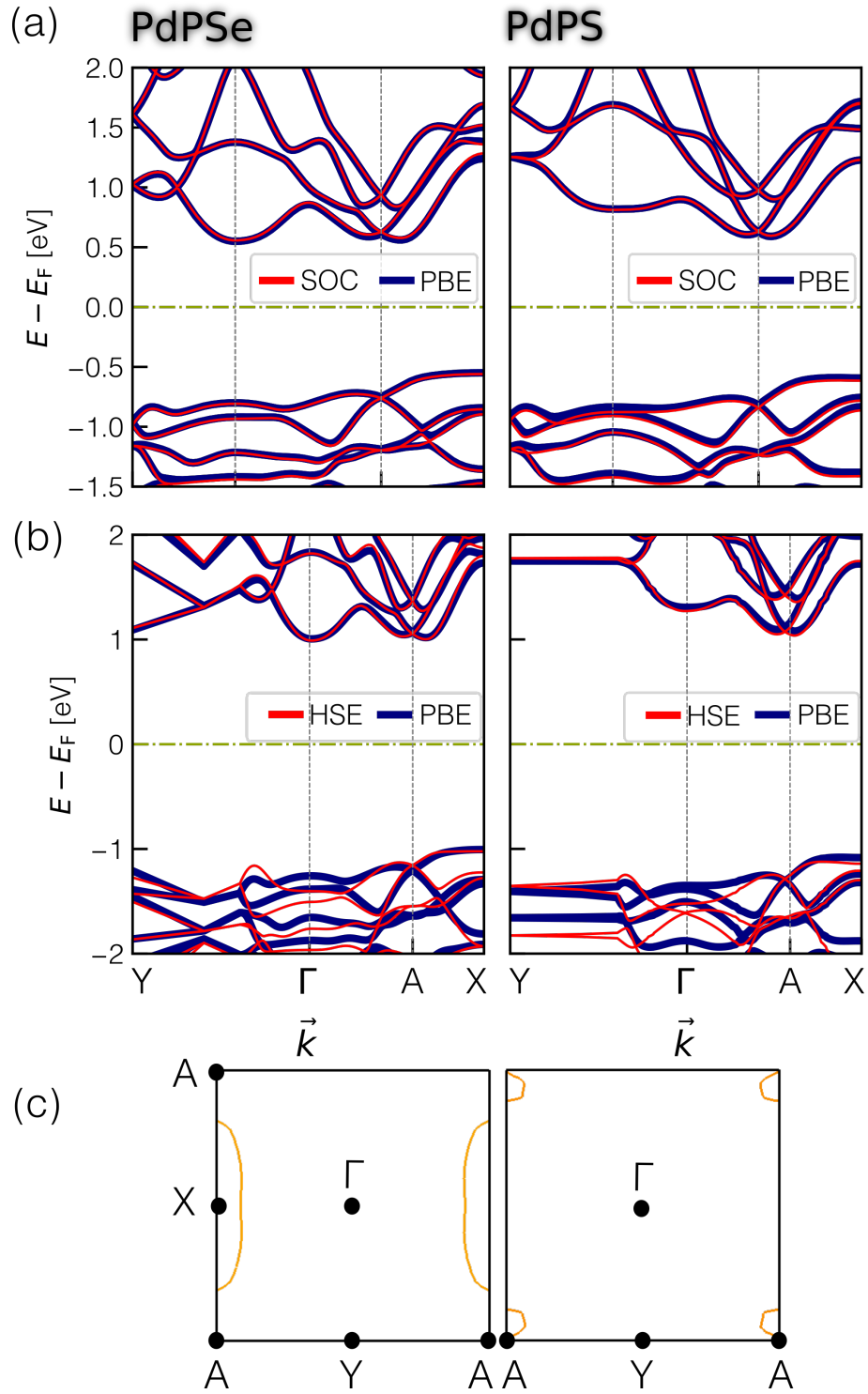


Fig. S2: a,b) Band structures of PdPSe and PdPS with and without including spin orbit coupling (SOC), and with different exchange correlation functionals, c) Fermi surface for PdPS around 36 meV above and below the Fermi level for valence band (left) and conduction band (right).

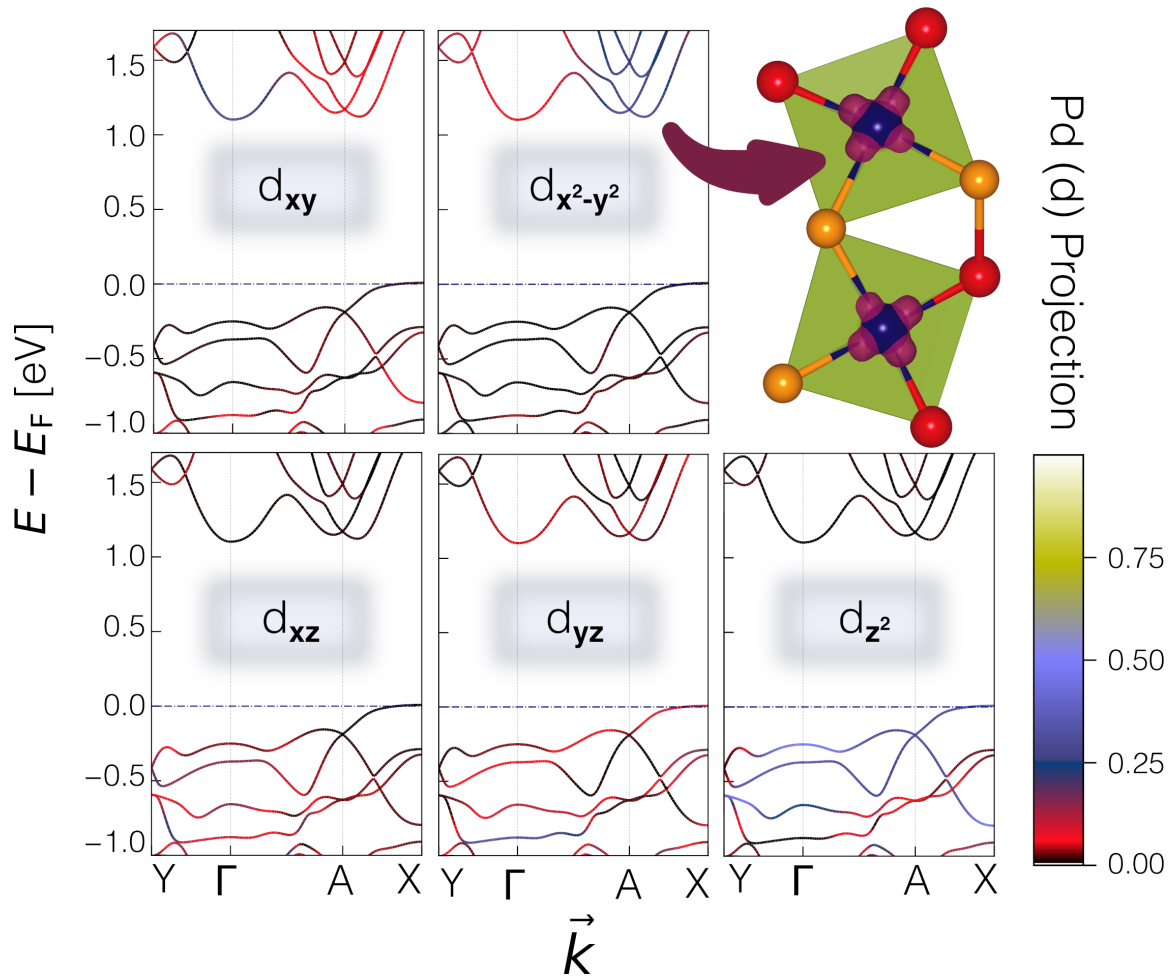


Fig. S3: PdPSe band structure with d orbitals projections. The contributions of $d_{x^2-y^2}$ and d_{xy} in conduction band and d_{z^2} in the valence band are predominant.

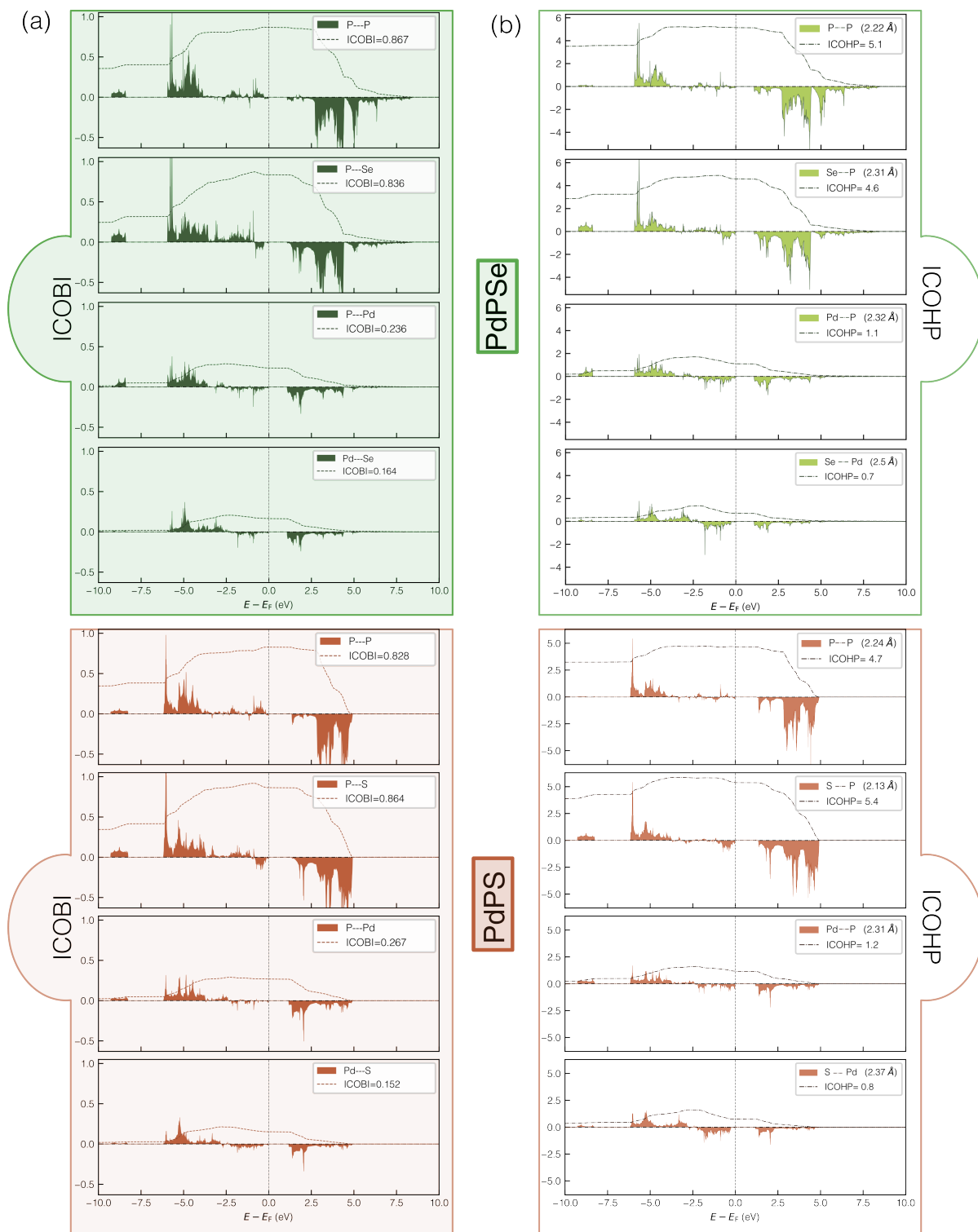


Fig. S4: COBI (crystal orbital bonding index) and COHP (crystal orbital hamilton population) analysis and their integration for PdPS and PdPSe. The high amount of COBI index is related to the covalent nature of P-Q and P-P bonding character and the low amount of COBI can be referred to the ionic bonds between Pd-P, Pd-Q.

Table S2: COBI, COHP, Bader and Born effective charges for PdPSe and PdPS. It is clear that anionic framework is bonded covalently within itself and it's linked to Pd ionically.

	Analysis	Pd-Q	Pd-P	P-P	P-Q	Pd	P	Q
PdPSe	ICOBI	0.164	0.236	0.867	0.836	—	—	—
	ICOHP	0.7	1.1	5.1	4.6	—	—	—
	Bader	—	—	—	—	0.02	0.19	0.20
	z^*	—	—	—	—	0.16	2.15	0.58
PdPS	ICOBI	0.152	0.276	0.828	0.864	—	—	—
	ICOHP	0.8	1.2	4.7	5.4	—	—	—
	Bader	—	—	—	—	0.12	0.27	0.48
	Z^*	—	—	—	—	0.14	2.19	0.96

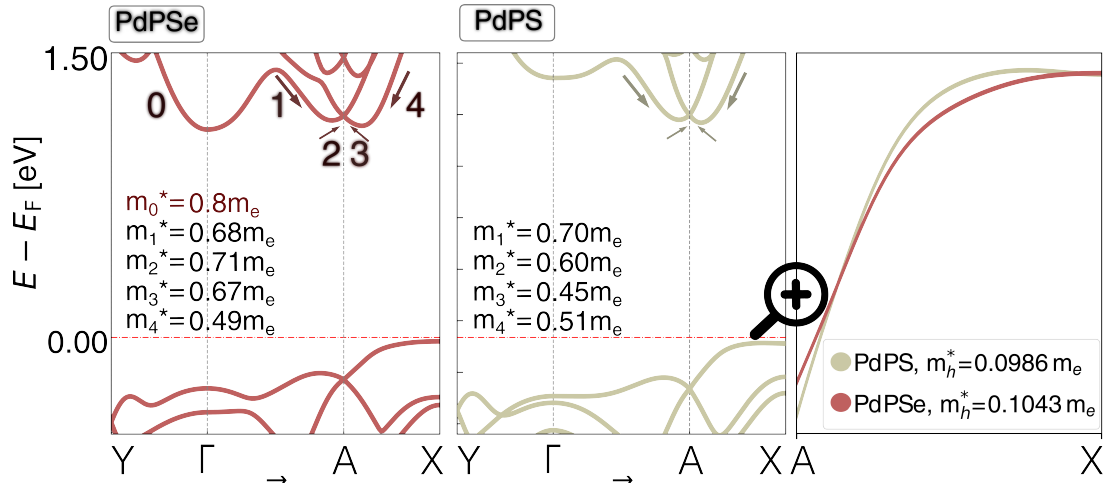


Fig. S5: Effective masses for different pathways in the band structures of PdPSe and PdPS compounds.

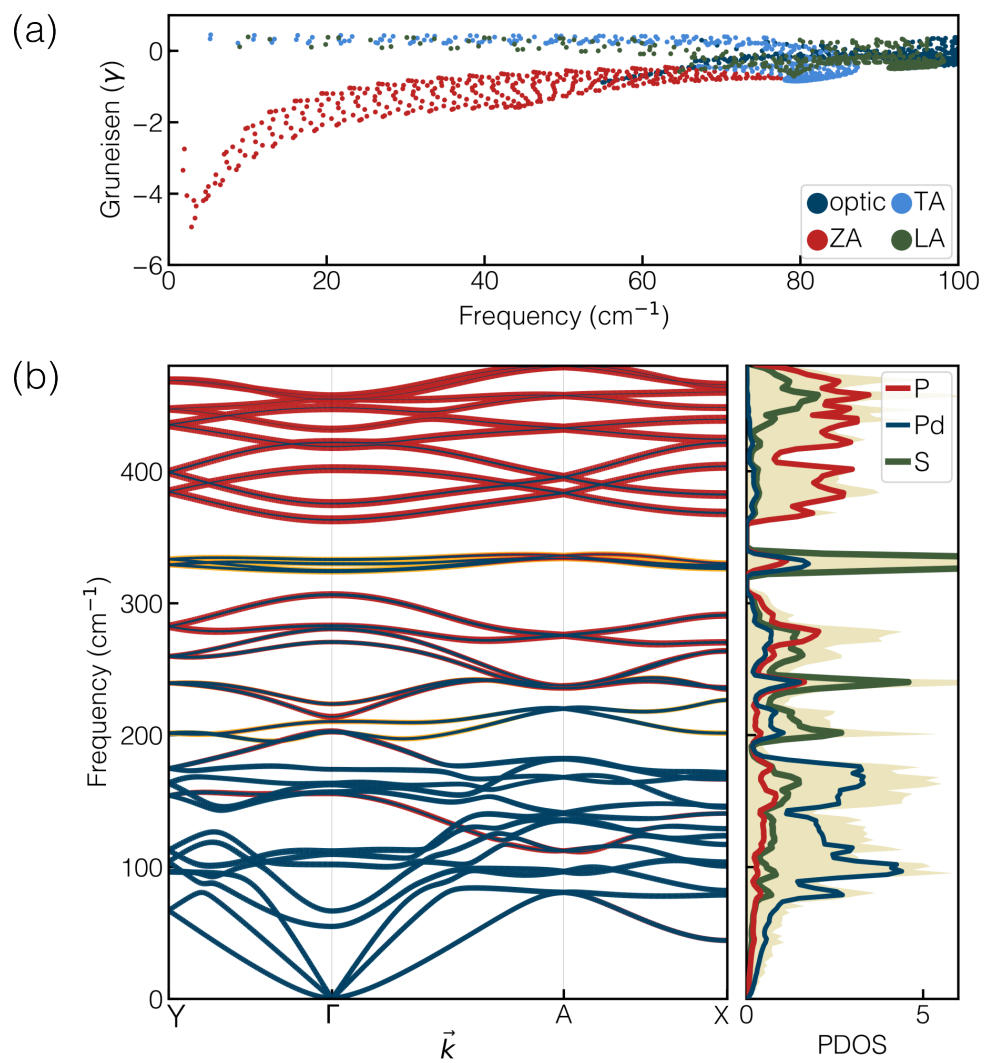


Fig. S6: Gruneisen parameter and phonon dispersion curve for PdPS.

Table S3: Calculated group velocities (ν_g) and Debye temperature (θ_D) of ZA, TA and LA phonons near the Γ point for the 2D-PdPQs along the a - ($X-\Gamma$) and b -directions ($Y-\Gamma$) compared with MoS₂.

MLs	CDs	ν_g (Km/s)			θ_D (K)		
		ZA	TA	LA	ZA	TA	LA
PdPS	a -axis	0.963	3.721	6.184	63.713	113.79	121.01
	b -axis	0.819	3.706	6.948	96.424	116.14	138.59
PdPSe	a -axis	0.766	3.253	5.094	51.693	89.059	99.076
	b -axis	0.774	3.237	5.922	80.193	96.198	110.99
MoS ₂	a, b -axis	1.40	3.96	6.47	257.90	257.90	326.98

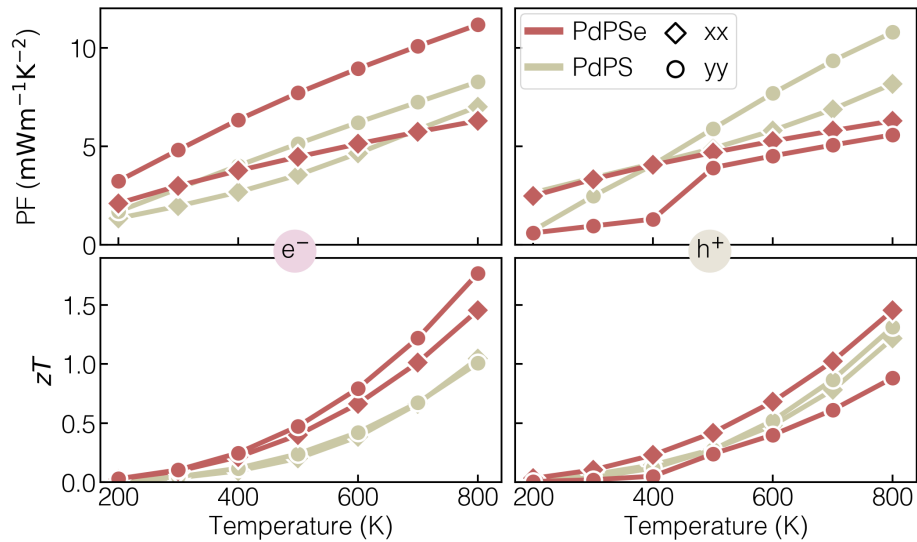


Fig. S7: Power factors and figure of merit for PdPSe and PdPS without including electronic relaxation time.

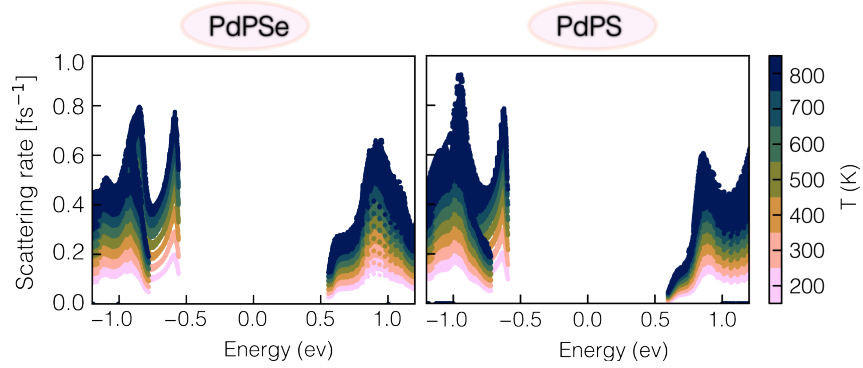


Fig. S8: Electronic scattering rates for PdPSe and PdPS calculated in different temperatures.

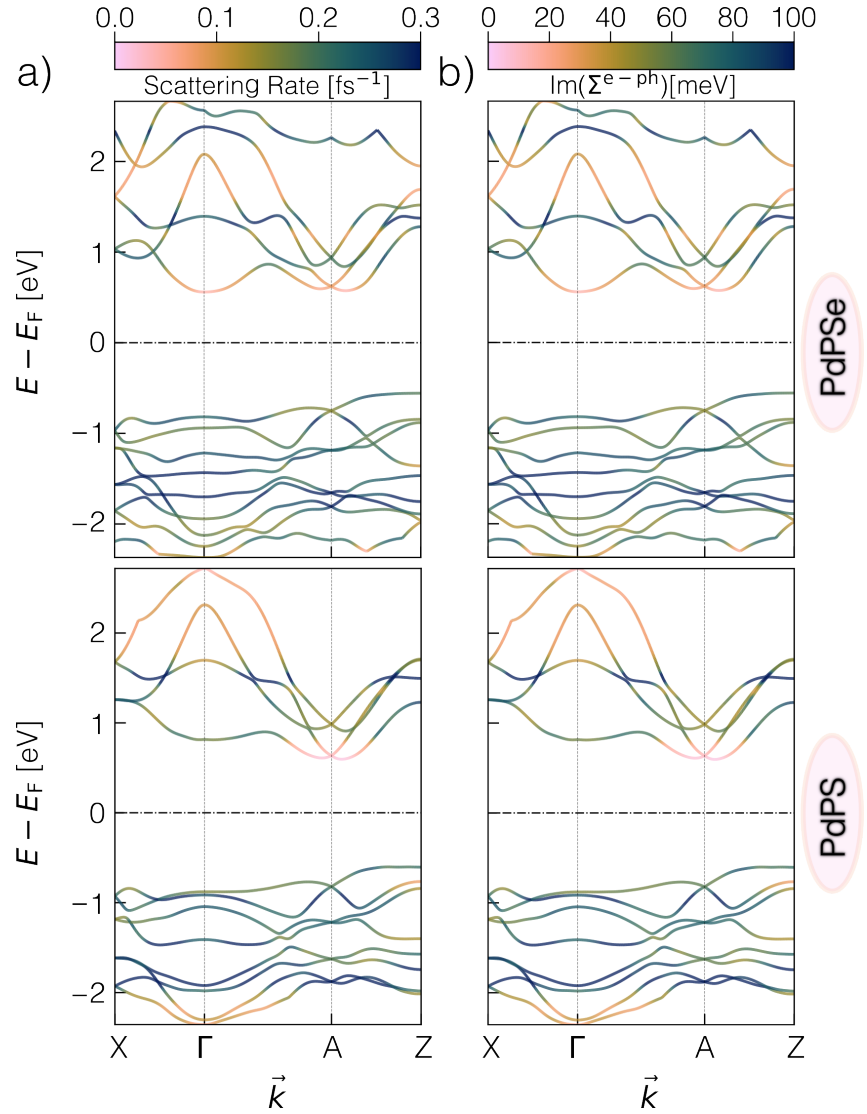


Fig. S9: Electronic scattering rates and relaxation times for PdPSe and PdPS calculated with ab-initio method.

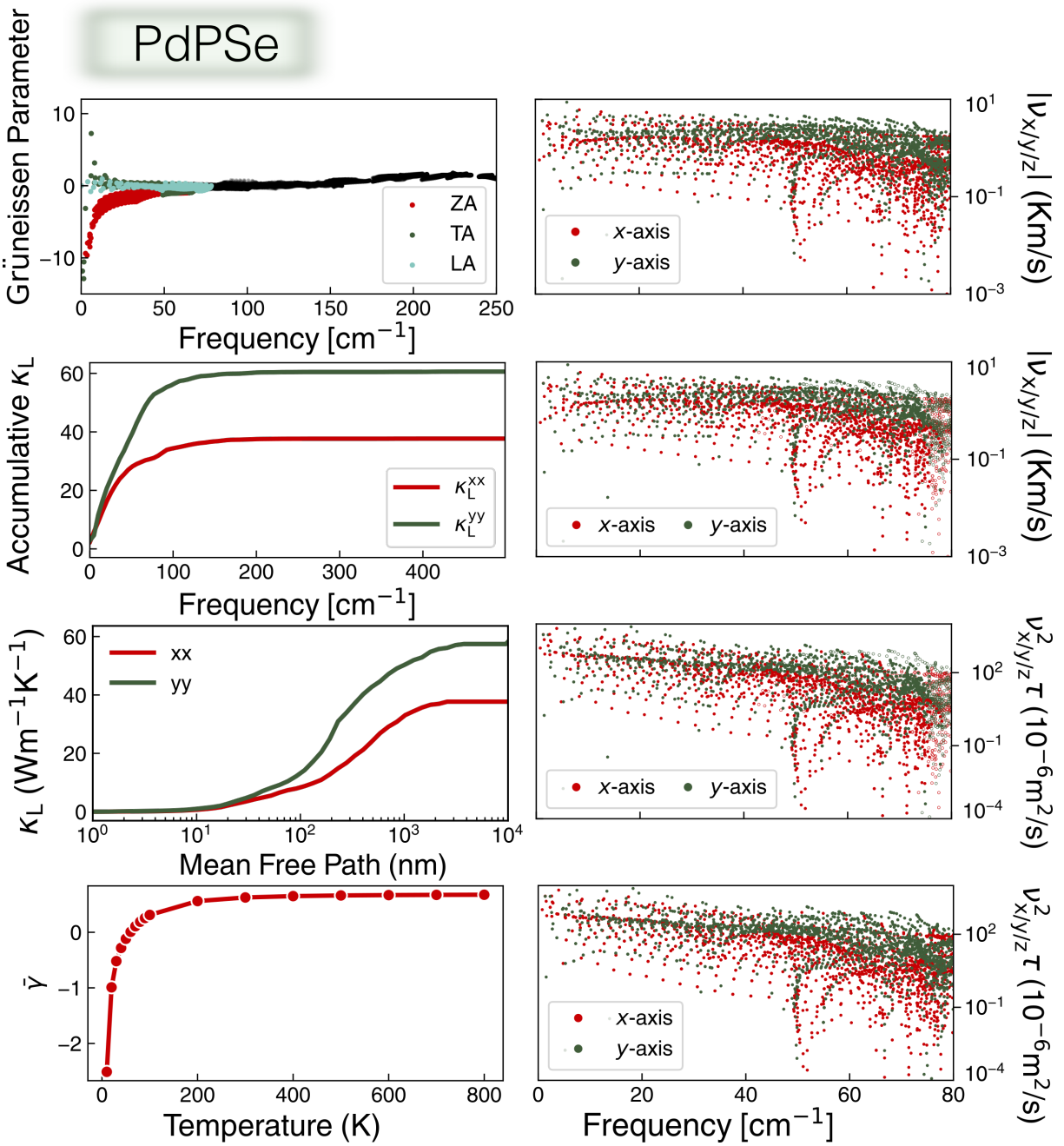


Fig. S10: ShengBTE Plots for PdPSe

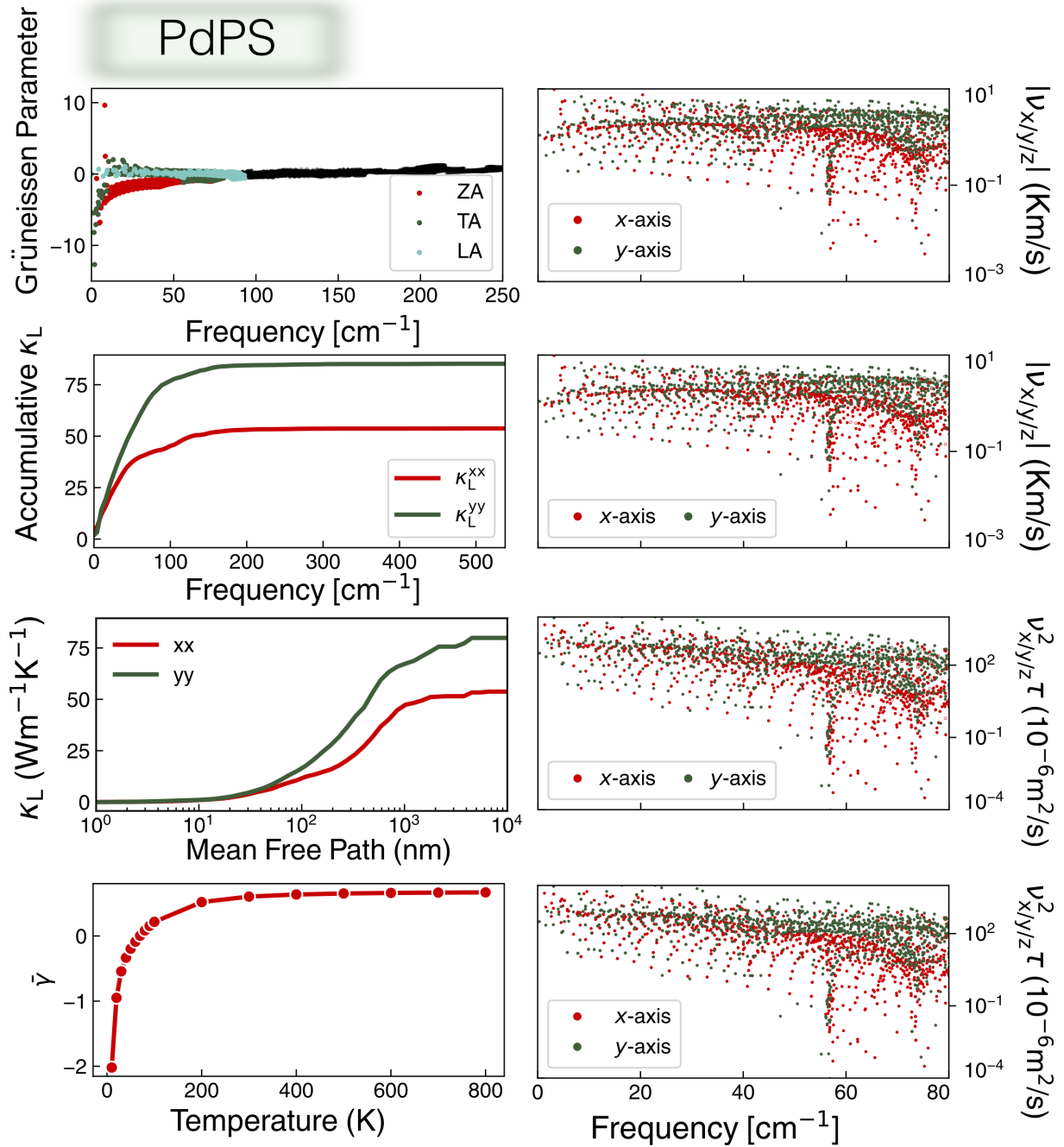


Fig. S11: ShengBTE Plots for PdPS

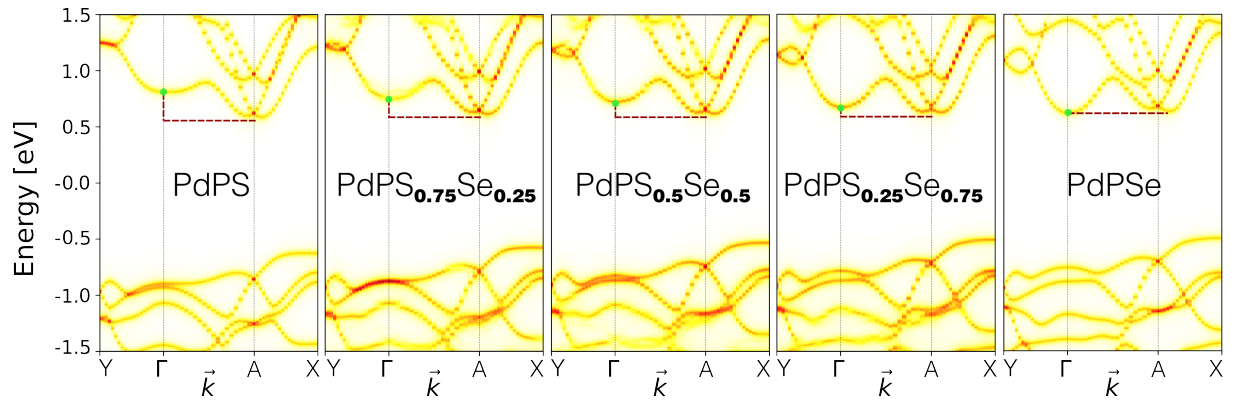


Fig. S12: Unfolded band structures for solid solutions. It is clear that the conduction band alignment is highly dependent to Se amount.

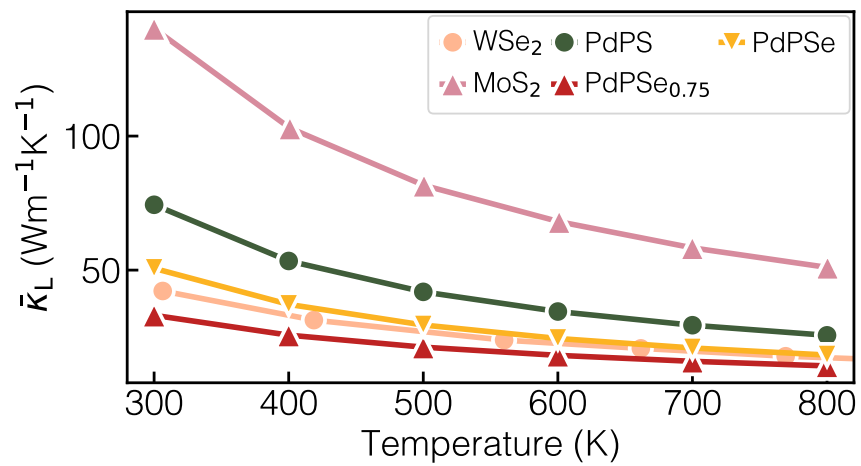


Fig. S13: Comparison between lattice thermal conductivities of 2D-transition metal dichalcogenides and 2D-PdPQs.

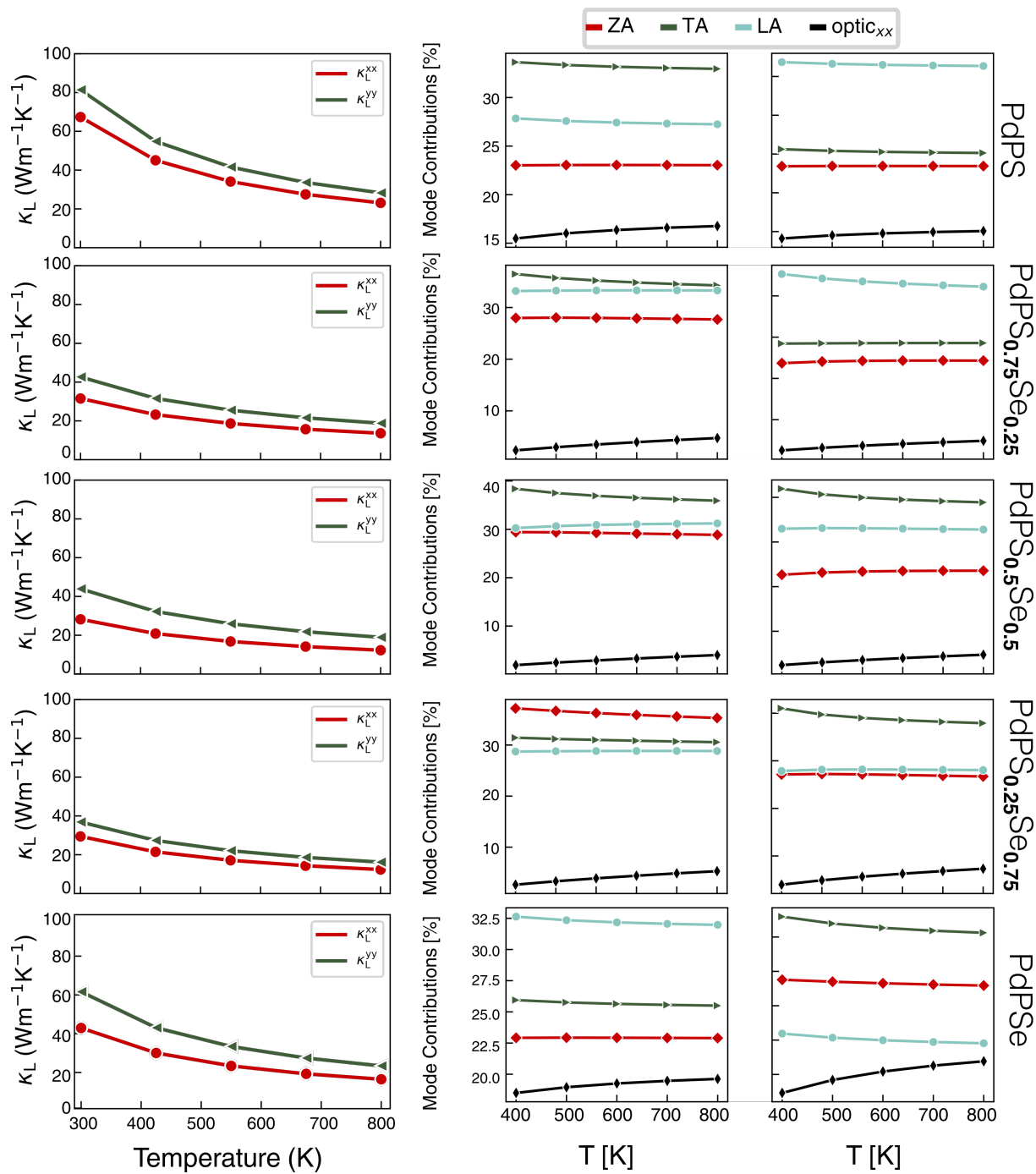


Fig. S14: Lattice thermal conductivities and their mode contributions for alloyed compounds.